Applied Physics A (2022) 128:894
https://doi.org/10.1007/s00339-022-06015-9

Applied Physics A
Materials Science & Processing

S.I. : COLA 2021/2022

Influence of multi-wavelength ultrafast laser texturing and autoclave sterilization on titanium alloy-based surface wettability

David Pallarés-Aldeiturriaga[1] · Steve Papa[2] · Alain Abou Khalil[1] · Alina Pascale-Hamri[3] · Mathieu Maalouf[2] · Yoan Di Maio[3] · Alain Guignandon[2] · Virginie Dumas[4] · Xxx Sedao[1,3]

Received: 2 June 2022 / Accepted: 24 August 2022 / Published online: 17 September 2022
© The Author(s) 2022

Abstract
Titanium alloys are widely used in bio-medical applications for their excellent bio-compatibility and superior mechanical strength. On the other hand, femtosecond laser processing is a robust versatile and industrial method widely used for surface functionalization. In this work, laser-induced periodic surface structures (LIPSS) on titanium alloy (Ti6Al4V) using different laser wavelengths of 1030 nm (IR), 515 nm (Green) and 257 nm (UV) were created and their surface wettability (physical parameter correlated with cell adhesion) was studied, in relation to sterilization process. The contact angle over LIPSS was smaller than over polished samples, with Green and UV LIPSS presenting contact angles inferior to 20° and a superior stability to sterilization process.

Keywords Ultrafast laser · Laser wavelength · Laser-induced periodic surface structures · Surface wetting · Sterilization · Bio-compatibility

1 Introduction

Femtosecond laser processing is a robust and industrial method widely used for surface functionalization allowing to enhance some properties of the materials [1–4]. Titanium and its alloys on the other hand are of great interest for processing. They exhibit excellent bio-compatibility and superior mechanical strength. Among the alloys, Ti6Al4V is of special interest as it is currently used for biological/biomedical applications, such as dental implants. This makes of high interest the laser texturing of such alloy; particularly, for aforementioned implants, where gingival fibroblasts adhesion is essential not only for implant support but also for its role as a physical barrier against bacterial infiltration, main reason of dental implant failure [5]. The inscription of laser-induced periodic structures (LIPSS) on metals increases surface functionalization [3, 6–9] which can enhance osseointegration of these titanium dental implants [10–13]. This is achieved thanks to the sensitivity of biological cells to nanoscale texturing, which makes them sensitive to LIPSS, as shown in the literature [4, 14]. There are other techniques, such as sandblasting or chemical treatment; however, they are not precisely controllable and require more complex and longer steps than in laser processing.

Wettability on the other hand is crucial to the cell adhesion properties, as cells are mostly known to prefer hydrophilic surfaces for a higher adhesion [15, 16]. In this work, the effect of ultrafast laser texturing and sterilization by autoclave over titanium based surface wettability is studied. Three different wavelengths of 1030, 515 and 257 nm were employed for LIPSS formation on Ti6Al4V surfaces, generating LIPSS periodicities of 760, 400 and 180 nm, respectively. Then, wettability tests were performed prior and post wet sterilization of the samples.

✉ David Pallarés-Aldeiturriaga
david.pallares.aldeiturriaga@univ-st-etienne.fr

[1] Hubert-Curien Laboratory, University of Lyon, Jean-Monnet University, UMR 5516 CNRS, 42000 Saint-Etienne, France

[2] Sainbiose Laboratory INSERM U1509, University of Lyon, Jean Monnet University, 42270 Saint Priest en Jarez, France

[3] GIE Manutech-USD, 20 rue Benoît Lauras, 42000 Saint-Etienne, France

[4] University of Lyon, Ecole Centrale de Lyon, Ecole Nationale d'Ingénieurs de Saint Etienne, Laboratory of Tribology and Systems Dynamics, UMR 5513 CNRS, 42100 Saint-Etienne, France

2 Setup

To inscribe LIPSS patterns with different periodicity, a classic processing setup composed of a femtosecond laser and a galvometric scanner was employed. A schematic of the setup is depicted in Fig. 1. The employed laser source for LIPSS at laser wavelength $\lambda = 1030$ nm was a "Tangor HP" from Amplitude lasers with $\tau = 400$ fs. The 515nm wavelength was obtained with the same laser and a nonlinear crystal to produce second harmonic generation. Finally, for 257 nm wavelength, a PHAROS and an HIRO Harmonic generation from light conversion were employed. The pulse duration was $\tau = 150$ fs. A $f-\theta$ lens was attached to the galvo scanner (intelliScan 14 from Scanlab for 1030 and 515 nm, and Thorlabs Dual-Axis Scanning Galvo Systems for 257 nm) to get homogeneous focal distance. The scan direction is also depicted in Fig. 1, where pulses were delivered with a separation Λ_x and a hatching distance Λ_y. The entire sample surface (10 $\times$ 10 mm) was texturized in this way. To achieve high quality and homogeneous LIPSS, a parametric optimization was performed. Table 1 summarizes the optimal parameters obtained that were employed for LIPSS inscription at each different wavelength. Within the scope of the current study, laser process parameters far apart from the ones listed above were observed to produce LIPSS with undesired effects or incomplete coverage.

Titanium alloy (Ti6Al4V) samples were purchased from Goodfellow. For surface roughness evaluation, both confocal microscope (Stil, from Altimet) and Atomic Force Microscope (AFM, from Brucker) were used, for large (10 $\times$ 10 mm) and localized (0.1 $\times$ 0.1 mm) surface topography measurements. The initial arithmetical mean height (Sa, the value of which varies in dependence of the surface area being considered) measured with the confocal microscope was 0.052 µm on the large surface area, and was 8.8 nm with AFM on the smaller and localized area.

One month after samples texturing, they were cleaned with an ultrasonic bath before wettability measurements were conducted. Wettability measurements were carried out with a laboratory-developed system within the MANUTECH-USD consortium. They were performed in a controlled atmosphere (temperature (T) = 22.95 $\pm$ 0.45 °C, relative humidity (RH) = 40 $\pm$ 8%). A 3 µL droplet of demineralized water was deposited on the surface, and the evolution of the droplet shape was visualized with a camera and a sample rotation stage enabling 360° inspection and contact angle measurements. The platform moved at a speed of 0.1 rad s^{-1}. The droplet profile and especially the contact angle (CA) were extracted from the complete droplet 360° rotation leading to approximately 80 measurements per droplet. The first CA measurements were carried out 1 month after laser processing and after an ultrasonic bath cleaning (demineralized water for 15 min). The second step of CA measurements was performed on the same samples, 24 h after a sterilization procedure in which the samples received an ultrasonic bath cleaning (demineralized water for 15 min), and an autoclave treatment at 134 °C for 19 min in specific bags, in accordance with dental implant industrial standards. The data represent the measurements from 4 consecutive, individuals and contact-less droplets on each surface.

Scanning electron microscopy (SEM) was used to visualize and characterize the different laser-induced patterns. A Tescan VEGA3 SB, Brno Czech Republic electron

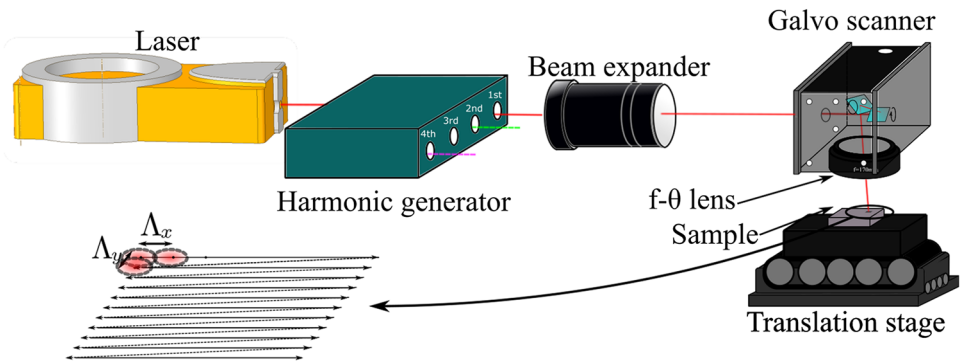

Fig. 1 Inscription setup and the scanning direction employed for texturization

Table 1 Optimized parameters for each wavelength

λ	F (J/cm^2)	PRR (kHz)	Λ_x (µm)	Λ_y (µm)	f (mm)	$2\omega_0$ (µm)
1030 nm	0.47	50	4	4	170	33
515 nm	0.45	50	4	4	88	28
257 nm	0.07	50	0.2	5	100	25

microscope was used operating at 20 kV and using the secondary electron detector.

3 Results and discussion

SEM micrographs of both control (polished) and laser processed (LIPSS) surfaces are shown in Fig. 2. An almost featureless morphology is observed from the polished sample surface. Traces of low contrast scratches are present due to the supplier polishing process. On the other hand, the LIPSS-covered surfaces show marked contrast due to the presence of surface topography variation of the periodic surface nanostructures. Since the scale is identical for all the 4 SEM micrographs in Fig. 2, the difference in periodicity of the LIPSS linked to the wavelength of the laser used is clearly observable: more precisely, the periodicity is 760 nm when the laser wavelength is 1030, 400 nm when the laser wavelength is 515, and 180 nm for a laser wavelength of 257 nm. For the sake of simplicity, the laser wavelengths shall be referred to as IR (1030 nm), Green (515 nm) or GR, and UV (257 nm) in the following text.

All laser-treated surfaces are relatively smooth (measured using the confocal microscope, the surface roughness Sa being 0.082, 0.058 and 0.158 µm for IR, Green and UV, respectively). The slightly raised value of Sa for the surface with UV LIPSS is attributed to the presence of a microscale undulation on the surface, which is presumably due to a large hatching distance Λ_y between successive laser scan tracks (that can be further optimized in the near future). To compare the polished, IR LIPSS and GR LIPSS surfaces (the Sa values of these surfaces are of tiny difference, revealed by confocal measurements) in further details, smaller areas of these surfaces are measured using an AFM. The 2D surface profiles obtained from AFM assessment are also presented in Fig. 2. One can see from these AFM measurements that surface Sa values derived from smaller areas (0.1 × 0.1 mm) are slightly different from those of the larger surface area measurement (10 × 10 mm) made by confocal microscope. It is also meaningful to mention that the amplitude of the LIPSS varies, depending on the laser wavelength (approximately 300 nm for IR LIPSS, 200 nm for GR LIPSS, and 100 nm for polished surface).

Once wettability evaluation protocol was performed, polished sample showed a high contact angle, as depicted in Fig. 3, resistant to sterilization process. It almost qualifies the polished Ti6Al4V as an hydrophobic (CA close to 90°) surface [17]. On the other hand, laser processing substantially reduces this angle by more than 60° presenting CAs inferior to 20°, especially with the lowest periodicity LIPSS (UV) showing the high hydrophilicity acquired by the surface due to femtosecond laser texturing process. There is

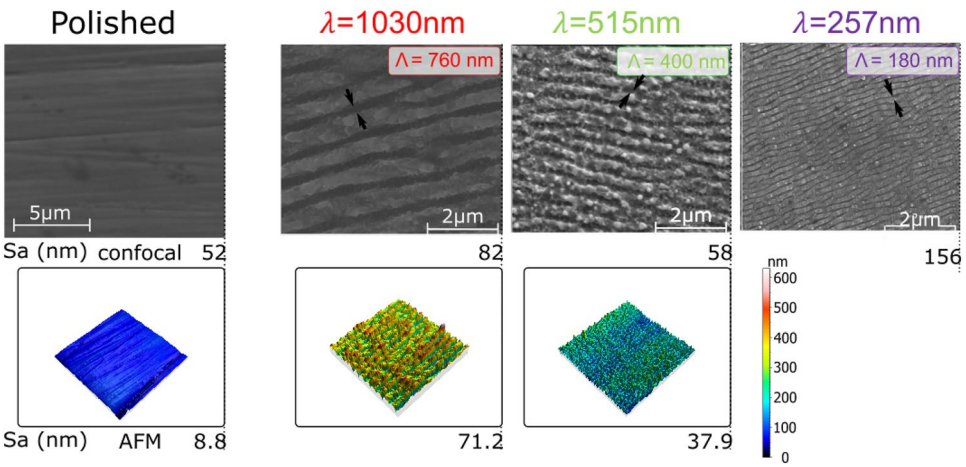

Fig. 2 SEM images and AFM surface profile of polished Ti6Al4V surface (left) and LIPSS induced at different wavelengths (right). Their ripple periodicity Λ and arithmetical mean height (Sa) measured by confocal microscope and AFM are shown above and bellow the images respectively

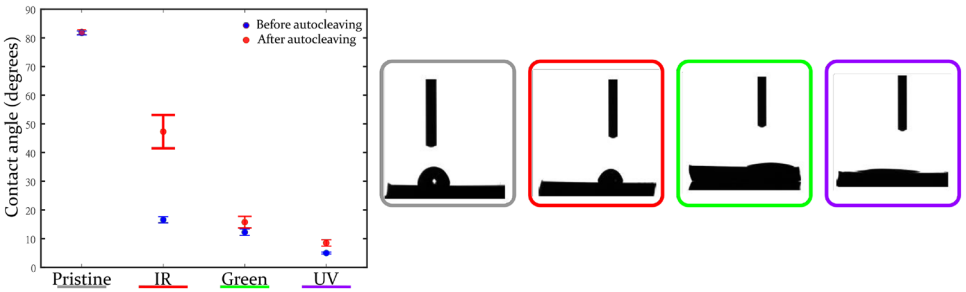

Fig. 3 Contact angle for polished and different LIPSS textured surfaces before and after sterilization process (left). Droplet images of Ti6Al4V surfaces after autoclave process (right)

a seeming tendency that lower CA values are achieved at LIPSS surface produced at shorter wavelength.

After sterilization process, CA of IR LIPSS was drastically increased by 30° reducing the wettability of the surface. By comparison, after same sterilization process, Green and UV LIPSS CAs were only increased by ≈ 3° each, showing the wetting stability of those two surfaces. It is worthwhile to mention that the water droplets do not appear to elongate along the LIPSS directions in all cases. Given the small periodicity and peak-to-valley amplitude of the LIPSS (compared to the mm-scale dimension of the droplets), the drops measured do not spread anisotropically.

In the current study, aside from the apparent surface morphology change induced by ultrafast laser irradiation at various laser configurations, the surface chemistry is also expected to be modified at the very same time, probably in different manners depending on laser conditions applied [18]. Superficial oxidation, thin amorphous layer formation Ti_xO_y, and microstructural defects formation in the underlying area are expected to occur [19, 20]. The formation and distribution of such phases are probably quite variable, depending on the wavelength deployed to form the LIPSS. Apart from surface microstructure modification itself, the surface reactivity after femtosecond laser irradiation may also play a role in the wettability modification process. Especially, the surfaces irradiated by ultrafast laser pulses at different wavelengths may have different affinity to surface adsorption of polar, non-polar C–O bonds containing species in the air, and hence great potential of behaving differently in surface wettability [21]. Dedicated surface chemistry analysis has not been pursued to de-correlate possible interplay between surface morphology change, surface chemistry change and resulting surface wettability, but this is definitely one of the key elements to investigate in the near future.

Despite the correlation between wettability and cell adhesion, biological experiments must be realised to confirm this behavior and to evaluate the impact of LIPSS periodicity on cell adhesion. As the most hydrophilic surfaces (Green and UV LIPSS) are not necessarily the best in terms of cell adhesion, an intermediate in terms of CA (IR LIPSS) may be a better compromise [22].

4 Conclusions

Laser-induced periodic surface structures were generated with three different laser wavelengths, namely, 1030 nm (IR), 515 nm (Green) and 257 nm (UV), presenting periodicity variation ranging from 760 to 180 nm. Wettability studies before and after clinical sterilization showed an enhanced wettability of Ti6Al4V samples after laser processing, for all LIPSS periodicity tested. Post-sterilization wettability tests also showed a stability of those hydrophilic properties for both Green and UV LIPSS which exhibited a minimal CA and negligible hysteresis for autoclave process. According to known preference of hydrophilic surfaces for cellular adhesion, ultrafast laser LIPSS texturing is of special interest for dental implant application.

Acknowledgements This project was co-funded by the European Union's Horizon 2020 research and innovation programme LaserImplant, under Grant Agreement Number: 951730; and a public Grant from the French National Research Agency (ANR) under the Investments for the Future Program (PIA): EUR MANUTECH SLEIGHT - ANR-17-EURE-0026.

Declarations

Conflict of interest The authors declare that they have no conflict of interest.

Open Access This article is licensed under a Creative Commons Attribution 4.0 International License, which permits use, sharing, adaptation, distribution and reproduction in any medium or format, as long as you give appropriate credit to the original author(s) and the source, provide a link to the Creative Commons licence, and indicate if changes were made. The images or other third party material in this article are included in the article's Creative Commons licence, unless indicated otherwise in a credit line to the material. If material is not included in the article's Creative Commons licence and your intended use is not permitted by statutory regulation or exceeds the permitted use, you will need to obtain permission directly from the copyright holder. To view a copy of this licence, visit http://creativecommons.org/licenses/by/4.0/.

References

1. E. Skoulas, A. Manousaki, C. Fotakis, E. Stratakis, Biomimetic surface structuring using cylindrical vector femtosecond laser beams. Sci. Rep. (2017). https://doi.org/10.1038/srep45114
2. E.K. Koussi, H.J. Jung, N. Faure, C. Donnet, C. Mauclair, X. Sedao, Comparative study of ultraviolet and infrared femtosecond laser irradiation on textile polymers PET and PA66. J. Laser Micro/Nanoeng. (2020). https://doi.org/10.2961/jlmn.2020.03.2015
3. X. Sedao, M. Lenci, A. Rudenko, N. Faure, A. Pascale-Hamri, J.P. Colombier, C. Mauclair, Influence of pulse repetition rate on morphology and material removal rate of ultrafast laser ablated metallic surfaces. Opt. Lasers Eng. **116**, 68–74 (2019). https://doi.org/10.1016/j.optlaseng.2018.12.009
4. A. Klos, X. Sedao, T.E. Itina, C. Helfenstein-Didier, C. Donnet, S. Peyroche, L. Vico, A. Guignandon, V. Dumas, Ultrafast laser processing of nanostructured patterns for the control of cell adhesion and migration on titanium alloy. Nanomaterials **10**(5), 864 (2020). https://doi.org/10.3390/nano10050864
5. S. Ferraris, F.T. Giachet, M. Miola, E. Bertone, A. Varesano, C. Vineis, A. Cochis, R. Sorrentino, L. Rimondini, S. Spriano, Nanogrooves and keratin nanofibers on titanium surfaces aimed at driving gingival fibroblasts alignment and proliferation without increasing bacterial adhesion. Mater. Sci. Eng. C **76**, 1–12 (2017). https://doi.org/10.1016/j.msec.2017.02.152
6. J. Eichstädt, G.R.B.E. Römer, A.J.H. in 'tVeld, Determination of irradiation parameters for laser-induced periodic surface structures. Appl. Surf. Sci. **264**, 79–87 (2013). https://doi.org/10.1016/j.apsusc.2012.09.120

7. A. San-Blas, M. Martinez-Calderon, J. Buencuerpo, L.M. Sanchez-Brea, J. del Hoyo, M. Gómez-Aranzadi, A. Rodríguez, S.M. Olaizola, Femtosecond laser fabrication of LIPSS-based waveplates on metallic surfaces. Appl. Surf. Sci. **520**, 146328 (2020). https://doi.org/10.1016/j.apsusc.2020.146328
8. M. Martínez-Calderon, A. Rodríguez, A. Dias-Ponte, M.C. Morant-Miñana, M. Gómez-Aranzadi, S.M. Olaizola, Femtosecond laser fabrication of highly hydrophobic stainless steel surface with hierarchical structures fabricated by combining ordered microstructures and LIPSS. Appl. Surf. Sci. **374**, 81–89 (2016). https://doi.org/10.1016/j.apsusc.2015.09.261
9. J. Bonse, Quo vadis lipss?—recent and future trends on laser-induced periodic surface structures. Nanomaterials (2020). https://doi.org/10.3390/nano10101950
10. M. Maalouf, A. Abou Khalil, Y. Di Maio, S. Papa, X. Sedao, E. Dalix, S. Peyroche, A. Guignandon, V. Dumas, Polarization of femtosecond laser for titanium alloy nanopatterning influences osteoblastic differentiation. Nanomaterials (2022). https://doi.org/10.3390/nano12101619
11. M. Muck, B. Wolfsjäger, K. Seibert, C. Maier, S.A. Lone, A.W. Hassel, W. Baumgartner, J. Heitz, Femtosecond laser-processing of pre-anodized Ti-based bone implants for cell-repellent functionalization. Nanomaterials (2021). https://doi.org/10.3390/nano11051342
12. E. Filipov, L. Angelova, D. Aceti, V. Marinova, D. Karashanova, A. Trifonov, I. Buchvarov, A. Daskalova, Altering the surface morphology and wettability of chitosan/graphene coatings by femtosecond and nanosecond laser processing. J. Phys. Conf. Ser. **2240**(1), 012041 (2022). https://doi.org/10.1088/1742-6596/2240/1/012041
13. A. Cunha, A.P. Serro, V. Oliveira, A. Almeida, R. Vilar, M.-C. Durrieu, Wetting behaviour of femtosecond laser textured Ti-6Al-4V surfaces. Appl. Surf. Sci. **265**, 688–696 (2013). https://doi.org/10.1016/j.apsusc.2012.11.085
14. R.Y. Siddiquie, A. Gaddam, A. Agrawal, S.S. Dimov, S.S. Joshi, Anti-biofouling properties of femtosecond laser-induced submicron topographies on elastomeric surfaces. Langmuir **36**(19), 5349–5358 (2020). https://doi.org/10.1021/acs.langmuir.0c00753
15. W. Song, J.F. Mano, Interactions between cells or proteins and surfaces exhibiting extreme wettabilities. Soft Matter **9**(11), 2985 (2013). https://doi.org/10.1039/c3sm27739a
16. L. Elena Sima, A. Bonciu, M. Baciu, I. Anghel, L.N. Dumitrescu, L. Rusen, V. Dinca, Bioinstructive micro-nanotextured zirconia ceramic interfaces for guiding and stimulating an osteogenic response in vitro. Nanomaterials (2020). https://doi.org/10.3390/nano10122465
17. K.-Y. Law, Definitions for hydrophilicity, hydrophobicity, and superhydrophobicity: getting the basics right. J. Phys. Chem. Lett. **5**(4), 686–688 (2014). https://doi.org/10.1021/jz402762h
18. J. Bonse, S. Gräf, Ten open questions about laser-induced periodic surface structures. Nanomaterials (2021). https://doi.org/10.3390/nano11123326
19. S.V. Kirner, T. Wirth, H. Sturm, J. Krüger, J. Bonse, Nanometer-resolved chemical analyses of femtosecond laser-induced periodic surface structures on titanium. J. Appl. Phys. **122**(10), 104901 (2017). https://doi.org/10.1063/1.4993128
20. X. Sedao, C. Maurice, F. Garrelie, J.-P. Colombier, S. Reynaud, R. Quey, G. Blanc, F. Pigeon, Electron backscatter diffraction characterization of laser-induced periodic surface structures on nickel surface. Appl. Surf. Sci. **302**, 114–117 (2014). https://doi.org/10.1016/j.apsusc.2013.10.152. E-MRS 2013 Symposium V: "Laser Material Interactions for Micro- and Nano-Applications" 27–31 May 2013, Strasbourg (France)
21. A.-M. Kietzig, S.G. Hatzikiriakos, P. Englezos, Patterned superhydrophobic metallic surfaces. Langmuir **25**(8), 4821–4827 (2009). https://doi.org/10.1021/la8037582
22. D.P. Dowling, I.S. Miller, M. Ardhaoui, W.M. Gallagher, Effect of surface wettability and topography on the adhesion of osteosarcoma cells on plasma-modified polystyrene. J. Biomater. Appl. **26**(3), 327–347 (2010). https://doi.org/10.1177/0885328210372148

Publisher's Note Springer Nature remains neutral with regard to jurisdictional claims in published maps and institutional affiliations.